2025 *Egypt. J. Chem.* **Vol. 67**, No. 7 pp. 319 - 329 (2027)

Egyptian Journal of Chemistry

http://ejchem.journals.ekb.eg/

Synthesis of zinc from spent zinc-manganese-carbon batteries and its application as sacrificial anodes in cathodic protection

M.M. Sadawy[1*], Saad. M. Fayed[1], Hani E. Sharafedin[1]

[1]Al-Azhar University, Faculty of Engineering, Mining and Pet. Dept., Nasr City, 11371, Cairo, Egypt

Abstract

The present study investigated the leaching of zinc from spent zinc manganese batteries in sulfuric acid solution and the synthesis of zinc anodes from the pregnant solution to be used for cathodic protection. The influences of acid concentration, liquid/solid ratio, stirring speed, and temperature on the dissolution rate were investigated. The leaching process of zinc from the batteries using sulfuric acid solutions achieved a high dissolution rate of approximately 97.3% within 60 minutes under specific conditions. The kinetic data for the leaching rate was analyzed and found to follow the chemical reaction-controlled process. Moreover, the electrochemical performance of the synthesized Zn anode obtained from the pregnant solution using electrodeposition and casting techniques was investigated. The results showed that the synthesized zinc anodes exhibited similar electrochemical performance to standard zinc anodes, with a current capacity of 736.23 A.h/Kg and an anodic efficiency of 89.79%. Further, the outcomes illustrated that the electrochemical performance of the synthesized Zn anode in artificial seawater obeyed the NACE Standard RP0169 potential criteria for cathodic protection.

Keywords*: Recycling; Spent batteries; Zinc–carbon battery; Heterogeneous reaction; Sulfuric acid leaching; Cathodic protection.*

1. Introduction

Batteries are devices that essentially transform chemical energy into electrical energy. The anode, cathode, electrolyte, separators, and external case are the main parts of batteries. Conventionally, batteries are classified into two main categories: (i) primary batteries (like alkaline manganese, zinc-carbon, mercury oxide, and silver oxide) and (ii) secondary batteries (such as nickel metal hydride, lead-acid, lithium-ion, and nickel-cadmium) [1]. The short lifespan of these batteries is the main disadvantage [2-4]. Zinc manganese-carbon batteries (ZMCB) contain zinc in the form of a can house as an anode, a graphite rod as a cathode, and an acidic electrolytic paste (a mixture of NH_4Cl, $ZnCl_2$, H_2O, and starch powdered graphite) to increase the conductivity and maintain moisture in the acidic electrolyte [5,6]. Typically, there is an asphalt seal as well as a plastic or paperboard separator. One of the biggest issues we currently have is the hazardous disposal of spent batteries, which poses an environmental risk owing to releasing heavy metals into the environment [7,8]. In fact, some types of batteries, like alkaline and zinc-carbon batteries, are compatible with municipal waste that has not been sorted [9]. As a result of the accumulation of large tonnages of waste, this causes a number of environmental issues that have an effect on the neighborhood. In terms of resource management, batteries may be regarded as a source of secondary raw materials [10]. Zinc, manganese, and steel are valuable metals that can be recovered and sold to make new batteries or other products [6]. Zinc-manganese-carbon batteries ought to be recyclable in an efficient, useful, and affordable way [11]. The primary and secondary zinc-containing materials may be treated using pyrometallurgical and hydrometallurgical procedures alone or in combination. However, when these processes are compared, the hydrometallurgical techniques are superior because of their better zinc recoveries for the materials with low zinc concentration.

Hydrometallurgical procedures are more economically viable and environmentally safe, in addition to several other operational benefits [12-14]. Recycling Zn metal from spent ZMCB as a secondary zinc-containing material is of great scientific, technological, and environmental interest [6]. Although a few methods for processing spent

*Corresponding author e-mail: mosaadsadawy@yahoo.com.; (M.M. Sadawy).
EJCHEM use only: Received date 26 October 2023; revised date 16 December 2023; accepted date 26 December 2023
DOI: 10.21608/EJCHEM.2023.244874.8781

batteries are in use, more efficient and less expensive alternatives are still required. For example, mineral processing techniques such as sorting, dismantling, magnetic separation, and grinding are typically the sequential steps involved in spent battery treatment. These pretreatment procedures are necessary to increase the metal dissolution rate in the aqueous solution [9].

Leaching spent ZMCB with H_2SO_4 solutions is the most common process, allowing attaining high zinc recoveries, commonly above 95% [15]. However, iron dissolves readily in this process and contaminates leachates [16]. Iron is a persistent challenge in ZMCB leaching [17]. The majority of the iron in batteries can be removed physically, but total separation is never easy to be obtained. As a result, the dissolved iron should be removed through precipitation [18]. On the other hand, Mn (in the oxidation state IV) is only soluble in acidic solutions in the presence of a reducing agent and its recovery is lower [19]. Numerous studies conducted by researchers revealed that while the amount of manganese solubilized by acid leaching is small, the range of values reached is wide, ranging from 5 up to 8% [9,18]. These procedures produce leachates that need additional purification before metal recovery because they have high zinc concentrations and low manganese concentrations [20,21].

The purification process will cost additional money and may be far from feasible [22]. So searching for new applications for this composition will reduce the cost. The synthesis of zinc from spent zinc-manganese-carbon batteries and its application as sacrificial anodes in cathodic protection fall under the economic sector of recycling and waste management. The recovery of valuable elements such as zinc, manganese, copper, and iron from spent batteries is essential for a circular economy and sustainability. Various processes have been developed for the selective recovery of these metals, including hydrometallurgical processes and pyrolysis [3-5]. The recovered metals can then be used in the production of new batteries or other applications, contributing to the reduction of waste and the conservation of natural resources [21,22]. For this reason, our study presents findings of spent zinc carbon battery pretreatments followed by dissolution tests in sulfuric acid solutions. The effects of various conditions, such as time of dissolution, acid concentration, dissolution temperature as well as the liquid/solid ratio were investigated. Further, the dissolution kinetic parameters had been calculated. On the other hand, the work was extended to manufacture Zn anode from the pregnant solution using electrodeposition and casting techniques. Further, the electrochemical performance of the synthesized Zn anode compared with a standard Zn anode was investigated in artificial seawater.

2. Experimental procedure

2.1 Material preparation

ZMCB with different sizes were collected from Al-Azhar University and different places. A series of mineral processing steps were performed according to Fig. 1. The batteries were crushed to (–1.0 cm) using a Jaw crusher (Model: Retch– type BB3 Masch. Nr 36323). The nonmetallic parts, such as papers and plastics, had been removed by hand sorting and dismantling. The remaining components were ground to a thickness of (-2.0 mm) using a disc crusher (Model: Bigo-Pulverised, Type UA), after which they were magnetically fractionated using a Frantz isodynamic separator type L-1 according to their magnetic susceptibilities at current intensities ranged from 0.05 to 1.0 ampere. After the spent ZMCB had been crushed and separated using magnetic separation, the non-magnetic material was washed and screened with a 2 mm sieve and dried in air at 105 ^{o}C for 24 h. The chemical composition of the powder is shown in Table 1.

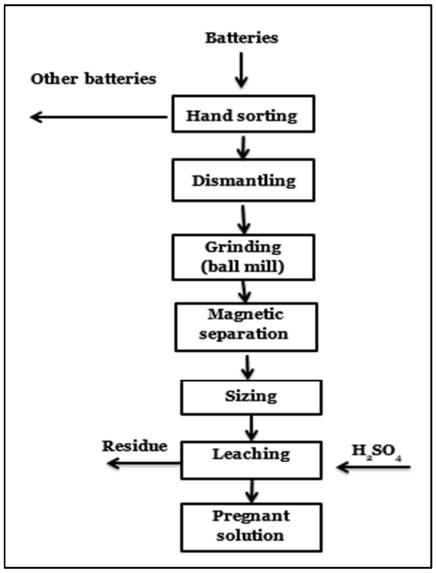

Fig. 1 Recycling flowchart of zinc spent batteries.

2.2 Leaching process

Different concentrations of H_2SO_4 solutions ranging from (0.5-2) M were prepared using analytical reagent grade and distilled water. Four factors were identified in this study namely, (acid

concentration, S/L ratio, stirring speed, and temperature). The product of each experiment was taken for the filtration process by vacuum to obtain the pregnant solution and analyze each to find the zinc recovered. The content of Zn in the pregnant solution was determined with EDTA titration and xylenol orange indicator [23]. The Zn dissolution content has been calculated using the following equation (1):

$$X_{Zn}\% = \frac{X_i}{X_t} \times 100 \quad (1)$$

where X_i is the content of zinc in the pregnant solution, and X_t is the total content of zinc in the sample. The reaction between sulfuric acid and zinc spent batteries was achieved in a 500 ml flask placed with a thermostatically controlled water bath.

Table 1 Chemical composition of the battery powder.

Element	Mn	Zn	Fe	Al	K	Cl	S	Si	Ca	Cd	Cr	Ni	LOI
Wt. %	47.88	32.56	1.04	1.21	0.52	0.33	0.3	0.21	0.21	0.14	0.11	0.04	14.46

Table 2 Chemical composition of the artificial seawater according to ASTM D1141.

Composition	NaCl	MgCl	Na_2SO_4	$CaCl_2$	KCl	$NaHCO_3$	H_3BO_3
g/L	24.53	5.20	4.09	1.16	0.69	0.20	0.02

2.3 Synthesis of zinc sacrificial anodes

The electro-deposition of Zn was performed using computer-controlled Potentiostat/Galvanostat (EG&G-273) in an electrochemical cell composed of stainless steel plate as a cathode with dimensions of (100×50×2) mm, Zn plate with dimensions of (100×50×0.5) mm as anode and Ag/AgCl reference electrode. The electrolyte volume was 500 cm^3, and the electro-deposition process was conducted in a 1000 cm^3 glass beaker. The Zn electrodeposits were prepared by applying a direct current of 0.10 A /cm^2 for 2 h. The obtained powders were washed with distilled water to remove the traces and air-dried at 105 ^oC. The powder was melted in a graphite crucible at 550 ^oC under nitrogen gas and poured into a steel mould (50 ×10× 5) mm. Finally, the mould was cooled naturally to ambient temperature.

2.4 Electrochemical corrosion tests

The Potentiostat/Galvanostatic (EG&G-273) was also used to conduct the electrochemical corrosion in artificial seawater having a chemical composition shown in Table 2. A three-electrode cell (Zn working electrode, platinum sheet counter electrode, and Ag/AgCl reference electrode) was utilized. The open-circuit potential (OCP) had been monitored directly after soaking the investigated anodes in the test environment for two days.

The potentiodynamic polarization test (PD) has been conducted with a contact surface area of 1.0 cm^2 and a scan rate of 0.15 mV/s. M 352 corrosion software program (EG&G Princeton applied research) was utilized for extracting the corrosion parameters. The corrosion rate (CR) in mmy^{-1} was determined using Eq. (2) [24]:

$$CR = 0.00327 \frac{Mi_{corr}}{\rho} \quad (2)$$

where M represents the equivalent weight (gram/equiv.), i_{corr} refers to corrosion current density ($\mu A/cm^2$), and ρ denotes the density of Zn (g/cm^3).

For Galvanostatic measurements, the anodes have been washed with acetone and deionized water before the test. With an anodic current density of 20 mA/cm^2, the Galvanostatic experiments were conducted for 2 hours. The mass loss approach was used according to ASTM G1&G31 [25]. The surface corrosion product has been removed from the corroded anodes by putting the anodes in a solution composed of (100 g ammonium persulfate /liter H_2O) for 5 min. The loss in weight was assessed using the weight difference to the nearest 0.1 mg *(Δ**W**)*. The current capacity and anode efficiency were measured according to ASTM G97 as follows in Eqs. (3,4) [26,27]:

$$C.C = \left(\frac{C}{W}\right) \quad (3)$$

$$A.E = \left(\frac{C.C}{820}\right) \times 100 \quad (4)$$

where *C.C* refers to the current capacity (Ah/kg), *C* characterizes the quantity of total charge passed, $\Delta\omega$ refers to the total weight loss, and 820 is the theoretical current capacity of pure Zn and A.E characterizes the anode efficiency [28].

To confirm that the results were repeatable, three different experiments were undertaken for each run. In each condition, the standard deviation has been calculated.

2.5 Surfaces characterization

X-ray diffractometer (XRD, Philips Analytical X-ray B.V. Machine) with monochromatic Cu-K radiation (λ= 0.154 nm) was utilized to determine the various anode phases. The scan values ranged from 10°-100° (2θ) with a scan rate value of 0.01°/ (2θ)/s. The XRD patterns were analyzed using the JCPDS database. The morphologies of anodes after (PD) test were examined using an Olympus optical microscope. At the same time, the morphologies after galvanostatic tests have been evaluated using a scanning electron microscope (model: SEM, JEOL JSM-5800LV).

3. Results and discussions

3.1 Leaching process

The chemical reactions that take place when zinc from spent zinc manganese batteries is introduced to the sulfuric acid solution can be expressed as follows in Eqs. (5-7) [29,30]:

$$Zno_{(s)} + H_2SO_{4(aq)} \rightarrow ZnSO_{4(aq)} + H_2O \quad (5)$$

$$Zn_{(s)} + H_2SO_{4(aq)} \rightarrow ZnSO_{4(aq)} + H_{2(g)} \quad (6)$$

The whole reaction can be written as:

$$Zno_{(s)} + Zn_{(s)} + 2H_2SO_{4(aq)} \rightarrow 2ZnSO_{4(aq)} + H_2O + H_{2(g)} \quad (7)$$

Fig. 2 reveals the effect of sulfuric acid concentration, in the range of 0.5-2.0 M, as a function of time at room temperature. The findings reveal that the zinc dissolution increases gradually with increasing time for all concentrations. However, the results show that the rate of dissolution increases with an increment in sulfuric acid concentration [31]. This is according to the potential-pH diagram for the zinc-water system shown in Fig. 3 is attributed to an increment of reactive concentration and reactive amount per surface area of zinc, eliminating zinc oxide coating which passivates the surface of zinc (Eq.5) and increasing Zn ions. After that, the chemical reaction between zinc and sulfuric acid increases and proceeds according to (Eq.7) [32]. For example, after 60 min, the dissolution increases from 6.8, 13.5, 19.8, and 23.1 % with increasing sulfuric acid concentration from 0.5 to 1.0, 1.5, and 2.0 M, respectively.

Choosing an appropriate liquid-solid (L/S) ratio is a key factor in enhancing the dissolution of Zn.

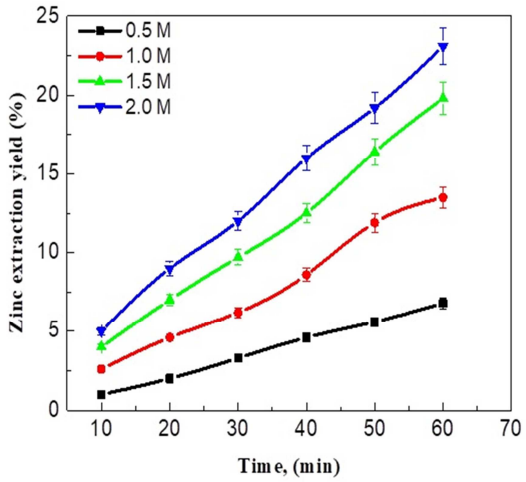

Fig. 2 Zinc leaching yields as a function of H_2SO_4 concentration.

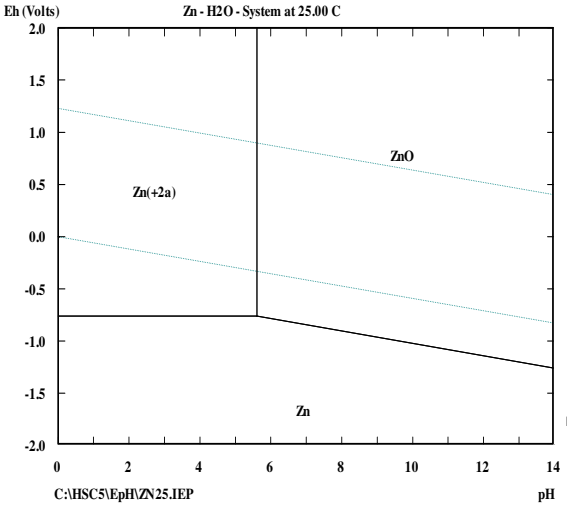

Fig. 3 Potentials- pH diagram for Zn-H_2O system at 25 ^{o}C.

Fig. 4 displays the effect of the L/S ratio on the leaching rate. Clearly, the outcomes show that the leaching rate increases with the increment of the liquid/solid ratio [33,34]. However, increasing the L/S ratio should decrease the metal ion concentration in the leaching solution and increase the leaching solution volume, which is unfavorable to the subsequent separation process. Therefore, the L/S ratio of 40:1 is suitable for the next operations.

Agitation is commonly essential to maximize kinetics and decrease the reaction times to make the process economically desirable. The variation of dissolution with respect to stirring speed over the range of 0–600 rpm in 2.0 M H_2SO_4 is given in Fig. 5. Clearly, the outcomes show that the dissolution rate is increased with the increment of stirring from 0 to 400 rpm. This can be because the batteries have a complicated composition. At low speeds cause the powder to partially disperse, causing the heavier metal particles to settle at the bottom of the beaker and be covered by the lighter nonmetal particles. This prevents the metal from fully contacting the leaching agent and lowers the mass transfer boundary layer thickness on the surface of the particles. Consequently, the outcomes show that by increasing the stirring speed to 400 rpm; the leaching solution's metal particles diffuse more quickly and bring fresh parts of H_2SO_4 into contact with the spent zinc battery, enhancing the leaching efficiency. However, the outcomes show that the stirring speed no longer has any discernible impact on the dissolution over 400 rpm. As a result, dissolution reached a steady state at 400 rpm, and this stirring speed was kept for subsequent tests [32].

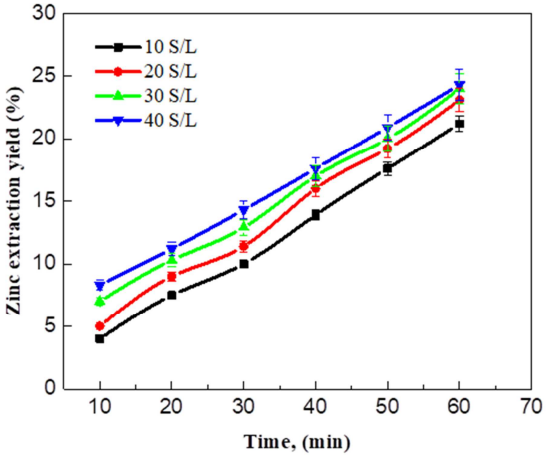

Fig. 4 Effect of the L/S ratio on Zinc leaching yields.

The impact of reaction temperature on the leaching of spent ZMCB was examined at a 30–90 ^{o}C temperature range in fixed conditions of (2M sulfuric acid concentrations, L/S ratio of 40:1, and stirring speed of 400 rpm). Fig. 6 demonstrates that the reaction temperature greatly affects the spent zinc battery dissolving rate. The leaching rate increases as the temperature rises. According to the Arrhenius equation, this behavior is due to the rate constant's exponential dependency. It is clear that the leaching rate of Zn increases from 24 to 97%. The dissolution rate can be increased with temperature rise, but the operation expense rises, and sulfuric acid severely evaporates, worsening the working conditions. Thus, 75 ^{o}C is determined to be the optimum temperature [35].

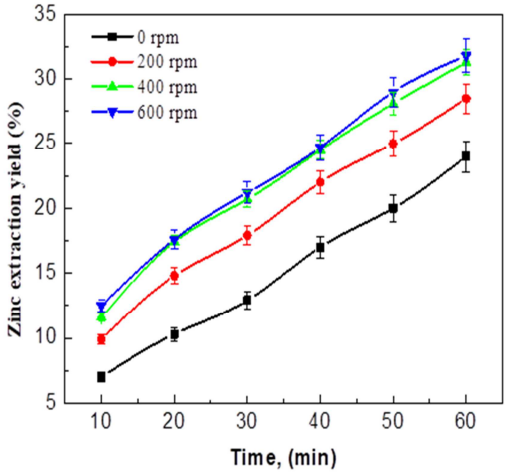

Fig. 5 Effect of stirring speed on Zinc leaching yields.

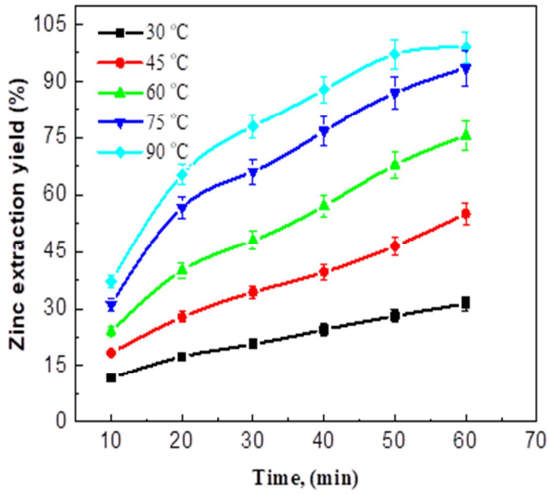

Fig. 6 Effect of temperature on Zinc leaching yields.

3.2 Leaching kinetics

Kinetic information is necessary to design and construct an efficient reactor in hydrometallurgical processes. Typically three processes control the rate of reaction in solid-liquid systems [36]: (i) film diffusion control (FDC), (ii) surface chemical reactions control (SCRC), and (iii) product layer (or ash layer) diffusion control (PLDC). The slowest of these sequential steps determines the process' total speed. The shrinking core model is used to examine experimental data in order to discover the kinetic parameters and rate-controlling process in the leaching of zinc in sulfuric acid solutions. This model, which may be described as follows in Eq. (8):

$$\alpha \text{ (liquid)} + b\ \beta \text{ (solid)} \rightarrow \text{Products} \quad (8)$$

The three control models can be written in Eqs. (9-11) as follows [4,12]:

i. Film diffusion control:

$$k.t = 1 - (1 - \theta)^{1/2} \quad (9)$$

ii. Surface chemical reactions control:

$$k.t = 1 - (1 - \theta)^{1/3} \quad (10)$$

iii. Product layer (or ash layer) diffusion control:

$$k.t = 1 - 3(1 - \theta)^{2/3} + 2(1 - \theta) \quad (11)$$

where θ is the fraction of the spent zinc dissolved; t stands for contact time (min), and k characterizes the reaction rate constant for the models (9) to (11). Using the aforementioned reaction models, statistical analysis was done to examine the kinetics of the reaction between a spent zinc battery and sulfuric acid. All the analyzed data was only connected to the relationship in Eq. (10), with a perfect correlation of roughly 0.998 after the three models were tested (Fig. 7).

3.3 Leaching activation energies

The activation energy of dissolving spent Zn can be obtained from the Arrhenius equation (Eq.12) [4,37]:

$$\ln K = \ln A - \left(\frac{E_a}{RT}\right) \quad (12)$$

where K characterizes the apparent rate constant, A refers to the pre-exponential factor, E_a is the energy of activation, R stands for gas constant, and T represents the absolute temperature (^0K). Plotting (ln K) versus ($1/T$), as shown in Fig. 8 a straight line with a slope ($-E_a/R$) and intercept ($ln\ A$) could be obtained. The E_a value was calculated from this equation and presented in Table 3.

It is known that the mathematical form of transition state theory for the Arrhenius equation may be written as shown in Eq.(13) [37]:

$$K = \left(\frac{RT}{Nh}\right)\exp\left(\frac{-\Delta H}{RT}\right)\exp\left(\frac{\Delta S}{R}\right) \quad (13)$$

where K is the apparent rate constant, (ΔH) refers to the enthalpy of activation, (ΔS) represents entropy of activation; N refers to Avogadro's number (6.022×10^{23}) molecule.mol^{-1} and h is Plank's constant (6.626×10^{-34}) J sec. Plotting ln(K/T) versus (1/T) as illustrated in Fig. 9, the slope of the line is ($-\Delta H/R$), and the y-intercept is ($\Delta S/R$). Table 3 also displays values of ΔH and ΔS.

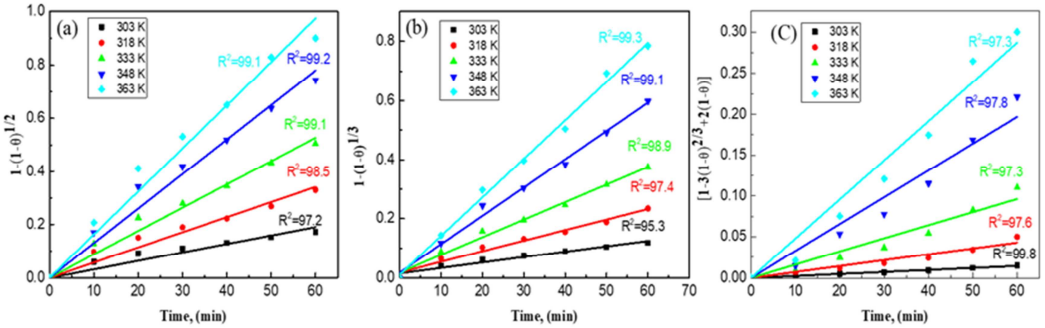

Fig. 7 Kinetic analysis for the leaching processes of Zn; (a) linear fitting of film diffusion control model, (b) linear fitting of the surface chemical reaction control model, and (c) linear fitting of product layer diffusion control model.

Table 3 Leaching kinetic parameters of ZMCB in H_2SO_4 solution.

ΔE, (KJ.mol^{-1})	ΔH, (KJ.mol^{-1})	ΔS, (kJ mol^{-1}K)	ΔE-ΔH
28.68	26.05	0.012	2.63

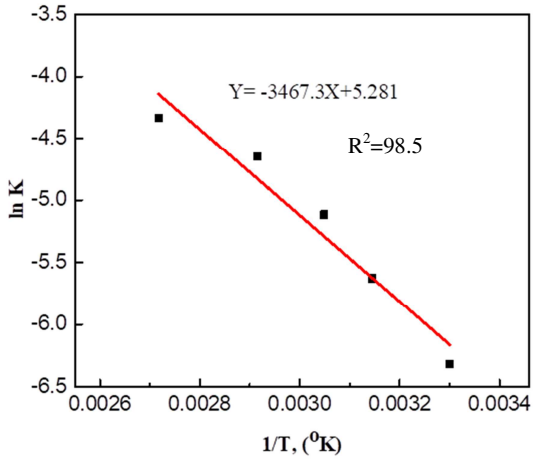

Fig. 8 Arrhenius plot for Zn dissolution in the chemical reaction control.

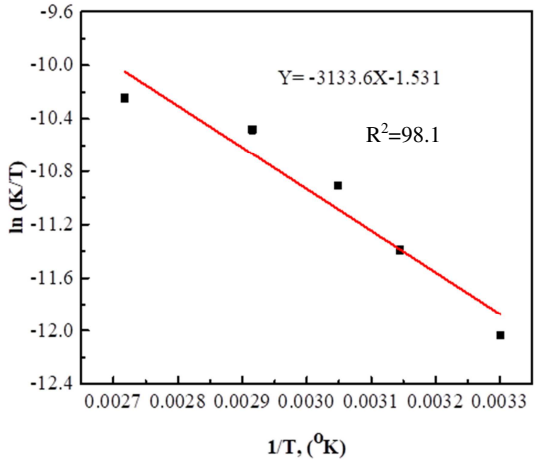

Fig. 9 Transition state plot for Zn dissolution in the chemical reaction control.

3.4 Electrodeposition of Zn from pregnant solution

Zn powders were deposited by applying a direct current of 0.10 A /cm^2 for 2 h into the pregnant solution. Fig. 10 shows the XRD peaks of Zn.

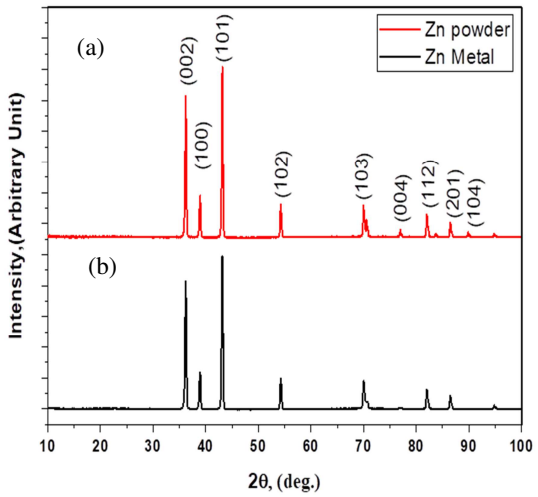

Fig. 10 XRD patterns of the synthesized Zn anode; (a) Powder and (b) cast anodes.

According to the Joint Committee of Powder Diffraction Standers (JCPDS) database, the reflection plans of the reflection planes of 36.29, 38.99, 43.22, 54.32, 70.07, 70.63, 77.04, 82.08, 83.75, 86.54, and 89.92 respectively, confirming the formation of a hexagonal Zn close-packed lattice structure. The powder was melted in a graphite crucible at 550 ^oC under nitrogen gas, poured into a steel mould, and cooled naturally to ambient temperature. Fig. 10 also shows the peaks of the cast Zn anode. The obtained XRD peaks of Zn confirm the formation of a hexagonal Zn structure.

3.5 Electrochemical corrosion tests

The open circuit potential (OCP) values of the synthesized Zn anode compared to the standard Zn anode were measured as a function of exposure time in artificial seawater. The OCP values of both anodes are given in Fig. 11. The initial value of the standard Zn anode is -1.009 V vs. Ag/AgCl; after 4, 16, 32, and 48 h, the OCP values shift to -1.047, -1.06, -1.095, and -1.105 V vs. Ag/AgCl, respectively. Further, the outcomes illustrate that the initial value of synthesized Zn anode is -1.002 V vs. Ag/AgCl and shifts to more negative values of -1.04, -1.06, -1.09, and -1.102 after 4, 16, 32, and 48 h, respectively. According to NACE *RP0169* criteria for cathodic protection, the value of 0.900 V vs. Ag/AgCl is the potential required to protect steel in seawater [38]. This means that the synthesized Zn is similar to the standard Zn anode and obeys the NACE criteria of cathodic protection.

On the other hand, the PD curves of synthesized Zn anode compared to standard Zn anode are shown in Fig.12. The plot contains cathodic and anodic

curves. The cathodic curves characterize the oxygen reduction on the surface of Zn anodes according to Eq. (14) [39]:

$$O_2 + 2H_2O + 4e^- \rightarrow 4OH^- \quad (14)$$

The anodic curves describe the dissolution of Zn anode according to Eq. (15) [40]:

$$Zn + 2H_2O \rightarrow Zn(OH)_2 + H_2 \quad (15)$$

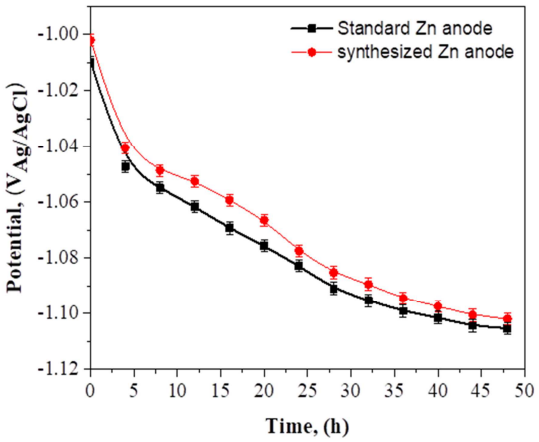

Fig. 11 Potential–time plot for the synthesized Zn anode compared with standard Zn anode in artificial seawater.

It can be observed from PD curves that the cathodic and anodic curves of the two anodes give similar polarization behavior and display a regular pattern. The electrochemical parameters deduced from Fig. 12 are summarized in Table 4. The obtained findings in Table 4 show that the electrochemical behavior of synthesized Zn anode is similar to standard Zn anode. Further, the corrosion rate of the synthesized Zn anode and standard Zn anode was found to be 0.322 and 0.279 mm/y, respectively.

The optical morphologies of the investigated anodes after PD tests are given in Fig. 13. The two anodes illustrate porous uniform corrosion products.

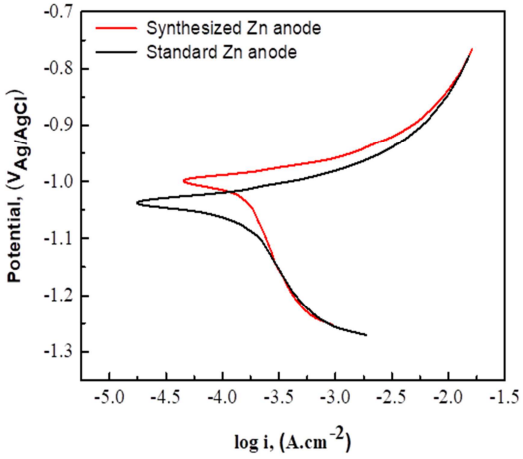

Fig. 12 Potentiodynamic polarization curves of the synthesized Zn and standard Zn anodes in artificial seawater.

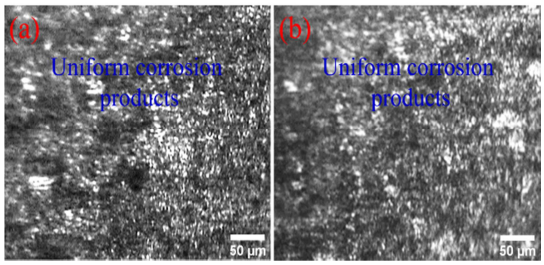

Fig. 13 Surface morphologies of the investigated anodes after potentiodynamic polarization tests in artificial seawater; (a) synthesized Zn and (b) standard Zn anodes.

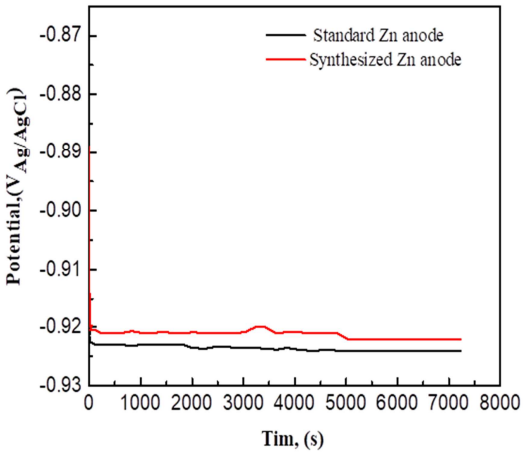

Fig. 14 Galvanostatic discharge plot for the synthesized Zn anode compared with standard Zn anode in artificial seawater.

Table 4 Electrochemical corrosion parameters obtained from potentiodynamic polarization test.

Anode	i_{corr} ($\mu A/cm^2$)	E_{corr} (mV)	Corrosion rate (mm/y)	$-\beta_c$ (mV/dec)	β_a (mV/dec)
Synthesized Zn anode	25.88	-997.6	0.322	234.42	119.51
Standard Zn anode	22.4	-1038.4	0.279	291.31	124.34

.

Fig. 14 gives the evolution of potential vs. immersion time for the investigated anodes at 20 mA/cm^2. Evidently, the findings illustrate that the process is classified into two stages: the first stage represents the decrease of potentials due to anodes dissolution, while the second stage characterizes the stability of the potentials due to the equilibrium between the anodes discharge and deposition of discharge products. Table 5 shows the anodic utilization and cell potential of the synthesized Zn anode compared to the standard Zn anode. Remarkably, the anodic utilization of the synthesized Zn anode is closed to the standard Zn anode. The SEM/EDS morphologies of the investigated anodes after the Galvanostatic test are revealed in Fig. 15(a,b). Clearly, the two morphologies illustrate loose and porous corrosion products. These loose products offer channels for reactive substances to transfer among the anodes and electrolytes. Therefore, the anodes preserve large reaction surfaces with negative potential and outstanding performance. Further, the relevant EDS analysis of the corrosion products is presented in Fig. 15 (a,b) [41-44].

Table 5 Galvanostatic anode characterization of synthesized Zn anode compared with standard Zn anode in artificial seawater.

Anode	Potential vs. Ag/AgCl (V)	C.C (A.h/Kg)	A.E
Synthesized Zn anode	-0.921	736.23	89.79
Standard Zn anode	-0.923	748.17	91.24

4. Conclusions

The synthesis of zinc from spent zinc-manganese-carbon batteries and its use as sacrificial anodes in cathodic protection were examined in the present work. The following are the key findings of this study:

i. The findings demonstrated that in 2 M H_2SO_4 at 75°C, approximately 97.3% of zinc was dissolved within 60 minutes using a liquid/solid ratio (L/S) of 40/1 and a stirring speed of 400 rpm. The kinetic data for the leaching rate was analyzed and found to follow a chemical reaction-controlled process. The energy of activation, enthalpy and entropy were 28.68 kJ/mol^{-1}, 26.05 kJ/mol^{-1} and -0.012 kJ $mol^{-1}K$ respectively.

ii. The corrosion rate of the synthesized zinc anode was determined to be 0.322 mm/y, with a corrosion current of 25.88 $\mu A/cm^2$.

iii. The electrochemical performance of the synthesized zinc anode, obtained from the pregnant solution using electrodeposition and casting techniques, was investigated and compared with a standard zinc anode. The outcomes illustrated that the electrochemical performance of the synthesized zinc anode in artificial seawater is similar to the standard zinc anode, indicating its potential for application in cathodic protection.

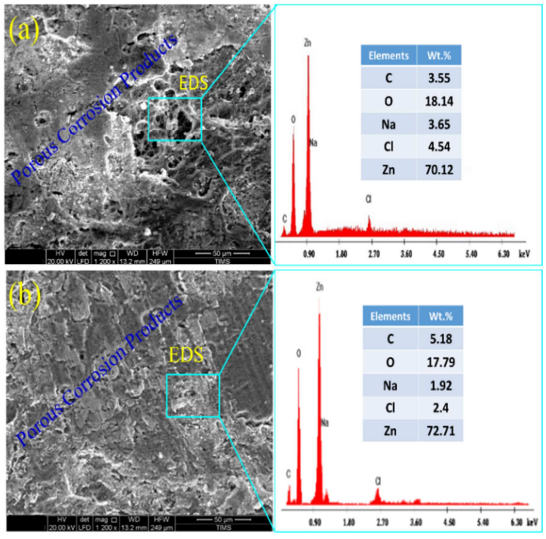

Fig. 15 Surface morphologies (SEM/EDS) of the synthesized Zn and standard Zn anodes after Galvanostatic tests in artificial seawater; (a) synthesized Zn and (b) standard Zn anodes.

Funding

The study did not receive funding.

Declarations

Conflict of Interest Statement: The authors confirm that there are no conflicts of interest between themselves, any individuals, or authorities involved in the study, and they solely own the research idea and its findings. Consequently, the authors declare the following: the article is original, written by the specified authors who are fully aware of its content and consent to its submission, it has not been previously published, it is not being considered for publication elsewhere, and no conflict of interest exists.

Ethical Approval Statement:

The study adheres to the principles of informed consent, and participants' consent to participate and consent to publish, when applicable, have been obtained following the prescribed procedures.

References

[1] A.M. Bernardes, D.C.R. Espinosa, J.A.S. Tenório, Recycling of batteries: A review of current processes and technologies, J. Power Sources. 130 (2004) 291–298.

[2] C.C.B. Martha De Souza, D. Corrêa De Oliveira, J.A.S. Tenório, Characterization of used alkaline batteries powder and analysis of zinc recovery by acid leaching, J. Power Sources. 103 (2001) 120–126.

[3] Sayilgan, T. Kukrer, N.O. Yigit, G. Civelekoglu, M. Kitis, Acidic leaching and precipitation of zinc and manganese from spent battery powders using various reductants, J. Hazard. Mater. 173 (2010) 137–143.

[4] J. Avraamides, G. Senanayake, R. Clegg, Sulfur dioxide leaching of spent zinc-carbon-battery scrap, J. Power Sources. 159 (2006) 1488–1493.

[5] Q. Li, X. Fei Rao, B. Xu, Y. Bin Yang, T. Liu, T. Jiang, L. Hu, Extraction of manganese and zinc from their compound ore by reductive acid leaching, Trans. Nonferrous Met. Soc. China (English Ed. 27 (2017) 1172–1179.

[6] C.A. Nogueira, F. Margarido, Selective process of zinc extraction from spent Zn-MnO_2 batteries by ammonium chloride leaching, Hydrometallurgy. 157 (2015) 13–21.

[7] A. Sobianowska-Turek, W. Szczepaniak, P. Maciejewski, M. Gawlik-Kobylińska, Recovery of zinc and manganese, and other metals (Fe, Cu, Ni, Co, Cd, Cr, Na, K) from Zn-MnO_2 and Zn-C waste batteries: Hydroxyl and carbonate co-precipitation from solution after reducing acidic leaching with use of oxalic acid, J. Power Sources. 325 (2016) 220–228.

[8] L.R.S. Veloso, L.E.O.C. Rodrigues, D.A. Ferreira, F.S. Magalhães, M.B. Mansur, Development of a hydrometallurgical route for the recovery of zinc and manganese from spent alkaline batteries, J. Power Sources. 152 (2005) 295–302.

[9] I. De Michelis, F. Ferella, E. Karakaya, F. Beolchini, F. Vegliò, Recovery of zinc and manganese from alkaline and zinc-carbon spent batteries, J. Power Sources. 172 (2007) 975–983.

[10] F. Ferella, I. De Michelis, F. Beolchini, V. Innocenzi, F. Vegliò, Extraction of zinc and manganese from alkaline and zinc-carbon spent batteries by citric-sulphuric acid solution, Int. J. Chem. Eng. 2010 (2010).

[11] G. Senanayake, S.M. Shin, A. Senaputra, A. Winn, D. Pugaev, J. Avraamides, J.S. Sohn, D.J. Kim, Comparative leaching of spent zinc-manganese-carbon batteries using sulfur dioxide in ammoniacal and sulfuric acid solutions, Hydrometallurgy. 105 (2010) 36–41.

[12] J. Zhao, B. Zhang, H. Xie, J. Qu, X. Qu, P. Xing, H. Yin, Hydrometallurgical recovery of spent cobalt-based lithium-ion battery cathodes using ethanol as the reducing agent, Environ. Res. 181 (2020) 108803.

[13] M.K. Jha, V. Kumar, R.J. Singh, Review of hydrometallurgical recovery of zinc from industrial wastes, Resour. Conserv. Recycl. 33 (2001) 1–22

[14] R.N.G. Guerra, C.A. Nogueira, F. Margarido, Leaching studies of spent zinc-manganese alkaline batteries with sulphuric acid, Mater. Sci. Forum. 587–588 (2008) 763–767.

[15] E. Sayilgan, T. Kukrer, F. Ferella, A. Akcil, F. Veglio, M. Kitis, Reductive leaching of manganese and zinc from spent alkaline and zinc-carbon batteries in acidic media, Hydrometallurgy. 97 (2009) 73–79.

[16] J.Y. Lee, Y. Pranolo, C.Y. Cheng, Z.W. Zhang, The recovery of zinc and manganese from synthetic spent-battery leach solutions by solvent extraction, solvent extr. Ion Exch. 28 (2010) 73–84.

[17] T. Skrzekut, A. Piotrowicz, P. Noga, M. Wędrychowicz, A.W. Bydałek, Studies of selective recovery of zinc and manganese from alkaline batteries scrap by leaching and precipitation, Materials (Basel). 15 (2022).

[18] F. Ferella, I. De Michelis, F. Vegliò, Process for the recycling of alkaline and zinc-carbon spent batteries, J. Power Sources. 183 (2008) 805–811.

[19] S.M. Shin, G. Senanayake, J. soo Sohn, J. gu Kang, D. hyo Yang, T. hyun Kim, Separation of zinc from spent zinc-carbon batteries by selective leaching with sodium hydroxide, Hydrometallurgy. 96 (2009) 349–353.

[20] M. Aaltonen, C. Peng, B.P. Wilson, M. Lundström, Leaching of metals from spent lithium-ion batteries, Recycling. 2 (2017).

[21] H. Shalchian, A. Rafsanjani-Abbasi, J. Vahdati-Khaki, A. Babakhani, Selective acidic leaching of spent zinc-carbon batteries followed by zinc electrowinning, Metall. Mater. Trans. B Process Metall. Mater. Process. Sci. 46 (2015) 38–47.
[22] R.N.G. Guerra, F. Pedrosa, F. Margarido, C.A. Nogueira, Metals recovery from spent Zn-MnO_2 batteries by hydrometallurgy, Proc. 2008 Glob. Symp. Recycl. Waste Treat. Clean Technol. REWAS 2008. (2008) 1039–1044.
[23] EDTA Titrations 1 : Standardization of EDTA and analysis of zinc in a supplement tablet by Professor David Cash September , 2008, (2008).
[24] S.M. Fayed, H. Wu, D. Chen, S. Li, Y. Zhou, H. Wang, M.M. Sadawy, Influence of positive pulse voltages on structure, mechanical, and corrosion inhibition characteristics of Si/DLC coatings, Surf. Coatings Technol. 445 (2022) 128749.
[25] S.M. Fayed, D. Chen, S. Li, M.M. Sadawy, E.A. Eid, Microstructure , mechanical , and electrochemical properties of Si / DLC coating deposited on 2024-T3 Al alloy, J. Alloys Compd. 966 (2024) 171452.
[26] ASTM Norma G 97, Standard test method for laboratory evaluation of magnesium sacrificial anode test specimens for underground applications, Annu. B. ASTM Stand. i (2008) 2–5.
[27] A. Elsayed, A. Nofal, G. Attia, Development of metal oxide incorporated Al-Zn-Sn sacrificial anodes processed by stir casting and heat treatment, J. Solid State Electrochem. 26 (2022) 2659–2672.
[28] J. Wen, J. He, X. Lu, Influence of silicon on the corrosion behaviour of Al-Zn-In-Mg-Ti sacrificial anode, Corros. Sci. 53 (2011) 3861–3865.
[29] S. Maryam Sadeghi, G. Vanpeteghem, I.F.F. Neto, H.M.V.M. Soares, Selective leaching of Zn from spent alkaline batteries using environmentally friendly approaches, Waste Manag. 60 (2017) 696–705.
[30] W.S. Chen, C.T. Liao, K.Y. Lin, Recovery zinc and manganese from spent battery powder by hydrometallurgical route, Energy Procedia. 107 (2017) 167–174.
[31] Yuliusman, R.A. Amiliana, P.T. Wulandari, M. Huda, F.A. Kusumadewi, Process optimization and leaching kinetics of zinc and manganese metals from zinc-carbon and alkaline spent batteries using citric acid reagent, IOP Conf. Ser. Mater. Sci. Eng. 333 (2018).
[32] R. May, zinc-carbon batteries using aqueous sulfuric, 46 (2011) 155–162.
[33] W.S. Chen, C.T. Liao, C.H. Chang, Recovery of Zinc and manganese from spent Zn-Mn batteries using solvent extraction, Key Eng. Mater. 775 KEM (2018) 427–433.
[34] T.H. Kim, J.G. Kang, J.S. Sohn, K.I. Rhee, S.W. Lee, S.M. Shin, Preparation of Mn-Zn ferrite from spent zinc-carbon batteries by alkali leaching, acid leaching and co-precipitation, Met. Mater. Int. 14 (2008) 655–658.
[35] I.G. Cruz-Reyes, J.A. Mendoza-Pérez, R. Ruiz-Guerrero, D.Y. Medina-Velázquez, L.G. Zepeda-Vallejo, Á. de J. Morales-Ramírez, Kinetics of Zn–C Battery Leaching with Choline Chloride/Urea Natural Deep Eutectic Solvents, Recycling. 7 (2022) 1–14.
[36] S. Kursunoglu, M. Kaya, Dissolution and precipitation of zinc and manganese obtained from spent zinc-carbon and alkaline battery powder, Physicochem. Probl. Miner. Process. 50 (2014) 41–55.
[37] S.M. Fayed, D. Chen, S. Li, Y. Zhou, H. Wang, M.M. Sadawy, Corrosion behavior and passive stability of multilayer DLC-Si coatings, Surf. Coatings Technol. 431 (2022) 128001.
[38] M. Sadawy, S. Saad, R. Abdel-Karim, Effect of Zn/Mg ratio on cathodic protection of carbon steel using Al–Zn–Mg sacrificial anodes, Trans. Nonferrous Met.
[39] L. Xu, Y. Xin, L. Ma, H. Zhang, Z. Lin, X. Li, Challenges and solutions of cathodic protection for marine ships, Corros. Commun. 2 (2021) 33–40.
[40] S.M. Fayed, D. Chen, S. Li, Y. Zhou, H. Wang, M.M. Sadawy, Corrosion behavior and passive stability of multilayer DLC-Si coatings, Surf. Coatings Technol. 431 (2022) 128001.
[41] M. Buzatu, S. Săceanu, M.I. Petrescu, G. V. Ghica, T. Buzatu, Recovery of zinc and manganese from spent batteries by reductive leaching in acidic media, J. Power Sources. 247 (2014) 612–617.
[42] M. Abbas, M.M. Sadawy, A.M. Hosny, Microstructure and electrochemical properties of Al-5Zn - 0.2Sn – 0.2Bi - xSb as a novel electrode for batteries applications, J. Alloys Compd. 923 (2022) 166303.
[43] S.F. Hameed, S. Rushdi, Z.T. Al-Sharify (2021) A Taguchi approach for optimization of mass transfer coefficient in metronidazole drug delivery process and activated carbon as a carrier, J. Eng. Res. 25–38.
[44] N.M. Almhana, S.A.K. Ali, S.Z. Al-Najjar, Z.T. Al-Sharify (2020) Assessment of cobalt ions removal in synthetic wastewater using broad bean peels, J. Green Eng. 10157–10173.